REPORT DOCUMENTATION PAGE

AFRL-SR-BL-TR-00-

0510

1. REPORT DATE (DD-MM-YYYY)	2. REPORT TYPE	3. DATES COVERED (From - To)
27-09-2000	Final	01 Apr 97 to 10 Oct 00

4. TITLE AND SUBTITLE

A Study of Hydrophilic Zones To Improve The Performance of Organic Coatings

5a. CONTRACT NUMBER

5b. GRANT NUMBER
F49620-97-1-0252

5c. PROGRAM ELEMENT NUMBER

5d. PROJECT NUMBER

5e. TASK NUMBER

5f. WORK UNIT NUMBER

6. AUTHOR(S)

D. Raghavan

7. PERFORMING ORGANIZATION NAME(S) AND ADDRESS(ES)

Howard University
Department of Chemistry
525 College Street, NW
Washington DC 20059

8. PERFORMING ORGANIZATION REPORT NUMBER

9. SPONSORING / MONITORING AGENCY NAME(S) AND ADDRESS(ES)

AFOSR/NL
110 Duncan Avenue Room B115
Boiling AFB DC 20332-8080

10. SPONSOR/MONITOR'S ACRONYM(S)

11. SPONSOR/MONITOR'S REPORT NUMBER(S)

12. DISTRIBUTION / AVAILABILITY STATEMENT

APPROVED FOR PUBLIC RELEASE: DISTRIBUTION UNLIMITED

13. SUPPLEMENTARY NOTES

14. ABSTRACT

Characterization of heterogeneous phases in polymers and hydrophylic regions in coatings have been the subject of AFOSR funded research project. Although hydrophilic regions occupy only a small fraction of the coating film volume, the hydrophylic regions control the corrosion protection performance of a polymer coating. At present the progress in the characterization of hydrophilic regions in coatings is very limited because of the lack of suitable analytical technique that can provide nanoscale lateral information. We mapped mechanical and chemical heterogeneities in model polymer coating compounds and characterized degradation susceptible regions in commercial coatings at nanoscale level. Nanoindentation procedure in combination with TMAFM was used to identify soft and hard regions in a heterogeneous model coating compound. To map chemically heterogeneous regions in model systems, we developed AFM/chemical modification approach. An effort was made to relate the microstructure of polymer coating film to the changes that occur to film upon environmental exposure and relate the changes to the chemistry of degraded compound. The material leached out from the coating during immersion was characterized. The leached material was mostly unreacted starting monomers and oligomers. They probably represent the degradation-susceptible regions (hydrophilic regions) of coating film. With the use of an atomic force microscope (AFM), which provides nanometer spatial resolution and angstrom depth resolution, we recently observed the progression of pathway formation in polyester and acrylic-polyurethane coatings, common protective materials for industrial, automobile, and aerospace applications. FTIR results in combination with AFM results (pit formation) support the observation that the extent of degradation of polyurethane coating film is much larger for samples exposed to UV at high relative humidities compared to no UV and high relative humidities or UV with low humidity.

15. SUBJECT TERMS

Hydrophilic, coatings

16. SECURITY CLASSIFICATION OF:			17. LIMITATION OF ABSTRACT	18. NUMBER OF PAGES	19a. NAME OF RESPONSIBLE PERSON
a. REPORT	b. ABSTRACT	c. THIS PAGE			19b. TELEPHONE NUMBER (include area code)
Unclas	Unclas	Unclas		39	

Heterogeneity of Polymer Film : Characterization and Protective Properties

D. Raghavan (PI)
Associate Professor
Polymer Science Program
Department of Chemistry
525 College Street, N. W.
Howard University
Washington, DC 20059

&

Tinh Nguyen (Collaborator)
Building Materials Division
National Institute of Standards and Technology
Gaithersburg, MD 20899.

Final Report Submitted to Dr. Charles Lee
AFOSR, Washington, DC

RESEARCH DEVELOPMENTS

If the durability of polymer coating is to be increased, it is essential to provide evidence that relates the regions in coatings that are susceptible to degradation in weathering environments to the hydrophilic regions in coatings. The hydrophilic regions are believed to range from nanometers to micrometers. At present the progress in the characterization of hydrophilic regions in coatings is very limited because of the lack of suitable analytical technique that can provide nanoscale lateral information.

The objective of this investigation was to provide an analytical technique that can map and identify the hydrophilic regions in polymer coatings. A coating has hydrophilic regions (that are believed to be mechanically soft and chemically polar material) that are present in a sea of hydrophobic material (that are believed to be mechanically hard and chemically nonpolar material). In this study, we initially characterize the hydrophilic and hydrophobic regions, by selecting a number of model polymer systems having known mechanical and chemical characteristics and then extend the study to characterize the degradation susceptible regions in a number of coating systems.

1) Nanoscale Characterization of Mechanical Heterogeneity of Coating Model Compounds

The first phase of this research was to develop a technique to characterize nanometer size, soft and polar domains in well defined polymer systems. In this study, tapping mode atomic force microscopy (TMAFM) and nanoindentation were used as analytical techniques to characterize nanodomains in polymeric systems. TMAFM was extensively used in this study because it provides a much better contrast on heterogeneity in materials than the conventional contact mode AFM. Since both surface mechanical and chemical properties of a polymer coating sample greatly affect the contrast of an TMAFM image, a number of model polymer systems were considered.

We initially made an attempt to understand the contribution of surface chemical and mechanical properties to phase image contrast by selecting a chemically and mechanically heterogeneous PMMA/PB blend system. The polarity of PMMA and PB were determined to be 0.146 and 0.009 respectively using contact angle measurements, and the T_g values for the pure PMMA and PB films were measured to be 102 °C and -105

°C, respectively. Thus, PMMA represents a glassy polar material and PB a soft non-polar material. Therefore, the unannealed PMMA/PB blends represent samples with chemical and mechanical heterogeneity.

In Figure 1a, AFM topographic (left) and phase (right) images are shown for a spin cast 20:80 blend film after 24 h of ambient conditioning (r_{sp} = 0.88). The thickness of this film was measured to be 375 nm ± 25 nm. Domain structures similar to patterns observed in phase-segregated polymer blends are observed in the topographic image. The 3-dimensional view of the topographic image is shown in Figure 1b. The average peak height for these domains is approximately 5.0 nm ± 0.5 nm. Some of the domains are elevated (brighter in color) while a few domains are depressed (darker in color) with respect to the surrounding area. Unlike in the topographic image, however, all the domain structures have the same dark color in the phase image while the surrounding matrix is distinguished by a relatively uniform bright color. This observation indicates that the contrast observed in the phase image is not significantly influenced by topographic variations. From the phase image, the average diameter of the domains was found to be approximately 0.42 μm ± 0.05 μm, where the average is calculated using images of several different areas. The spacing of these domains was found to vary from area to area.

To identify the domain and matrix regions as PB-rich and PMMA-rich or visa versa, the nanoscale indentation response of the different regions of each blend were studied using the AFM in force mode. In the force-distance curves for pure PMMA and pure PB films (not shown), tip penetration into the PB was significantly larger than for the PMMA, which correlates to the lower stiffness of the soft PB compared to the glassy PMMA. Also, the larger tip penetration results in a larger contact area between the tip and the sample, which increases the adhesive pull-off force. Using the same tip and experimental conditions as used for the pure films, force-distance curves were measured for the domains and the surrounding matrix in each of the blends. The force curves for the dark phase domains and bright phase matrix of the 20:80 blend are shown in Figures 2a and 2b, respectively. A force curve can be divided into the repulsive region and the attractive region, where the repulsive region is characterized by positive tip deflection

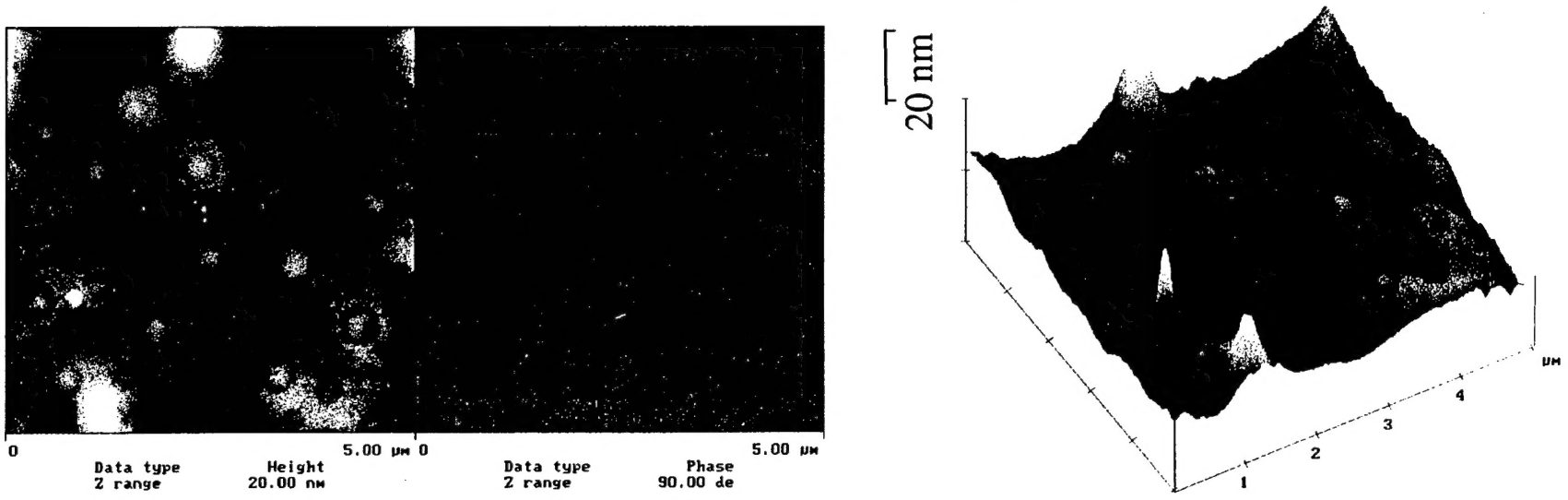

a b

Figure 1 (a) Tapping mode AFM height image (left) and phase image (right), and (b) a 3-dimensional representation of the topography for the 20:80 blend after 24 h of ambient conditioning (r_{sp} = 0.88). Contrast variations are 20 nm from white to black for the height images and 90 ° from white to black for the phase image.

values and the attractive region is characterized by negative tip deflection values. Note that the horizontal portion of the force curve on the right half of both plots in Figure 2 corresponds to zero tip deflection, as the tip is well above the sample surface and no tip-sample interaction is occurring. The slope of the repulsive region for the dark domain (see Figure 2a) is steeper than that for the surrounding matrix (see Figure 2b) for both the extending and retracting curves. Further, for the dark domains, the trough in the attractive region is shallower than that for the surrounding matrix such that the adhesive pull-off force is less. These observations indicate that the amount of tip penetration into the dark domain is less than for the matrix. Further, the differences in the force curves for the domains and the matrix are similar to the differences between force curves for pure PMMA and pure PB discussed previously. Similar results were obtained for the 80:20 and the 50:50 blend samples. Using these results, the dark domains of the phase images in Figures 1 are likely to be PMMA-rich regions and the bright matrix surrounding the domains is likely to be rich in PB.

To verify that domain in PMMA/PB blend is indeed PMMA rich region, we performed compositional analysis using images of blends with different concentrations. Computer image analysis was used to measure the area fraction of the dark contrast regions for each of the blend samples. For these measurements, three 20 μm x 20 μm images of each film were analyzed. For the 20:80 blend, the area occupied by the domains is approximately 24 % ± 3 % of the scan area, while that for the 50:50 blend is approximately 39 % ± 9 % of the scan area and that for the 80:20 blend is approximately 69 % ± 7 % of the scan area. Although only a few small areas of each sample were analyzed, the area fraction of the darker domains seems to increase with increasing composition of PMMA in the blend. Thus, the identification of the domains as PMMA-rich regions using image analysis agrees with the force curve results.

As mentioned previously, PMMA and PB regions in unannealed PMMA/PB system differ significantly in both mechanical and chemical properties. However, by controlled annealing, we found that the chemical differences and the mechanical differences of the PMMA/PB system can be minimized. Thus, changes in the blend samples was studied as a function of annealing to investigate the effects of surface

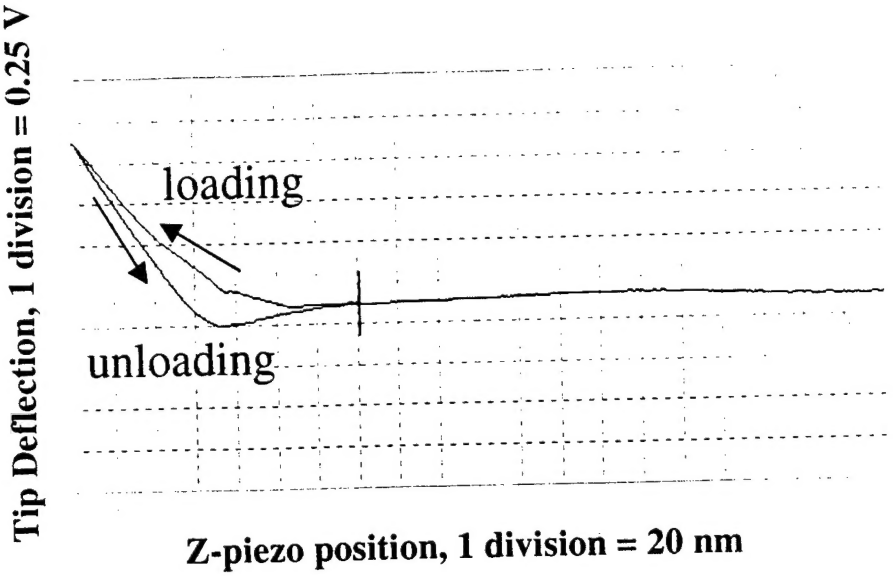

(a)

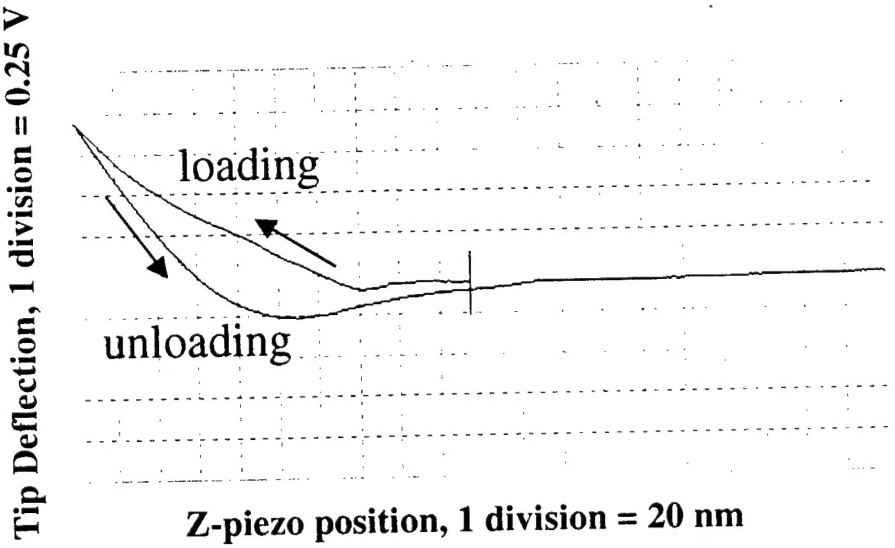

(b)

Figure 2 Typical force curves for (a) the domain region (darker color in the phase image) and (b) the matrix (brighter color in the phase image) for the 80:20 blend after 24 h of ambient conditioning.

property differences on phase image contrast and force-distance curves. This information would be very useful in the characterization of hydrophilic regions in a sea of hydrophobic polymer.

In Figures 3a-3d, topographic (left) and phase (right) images of the 20:80 blend are shown for annealing times of 0 h, 5 h, 20 h, and 107 h, respectively, where the images shown in Figure 3a are the same as in Figure 1a. The morphology of the blend, i.e., circular PMMA-rich domains in a PB-rich matrix, does not change with annealing. However, the phase contrast between the domain and matrix regions decreases with increasing annealing time. In fact, after 107 h of heating (see Figure 3d), the phase values of the domains and the matrix are approximately the same. Also, the heights of the PMMA-rich domains increase with respect to the PB-rich matrix with increasing annealing time. The phase image contrast of PMMA/PB blend films decreased with increasing annealing time. In fact, after annealing for 107 h, the phase image contrast between PMMA-rich domains and the PB-rich matrix is negligible, as shown in Figure 3d. The only remaining contrast in this figure is caused by the sensitivity of the phase of the oscillating probe to the topographic differences between the domain edges and the surrounding matrix, which has been enhanced due to the shrinkage of the matrix with annealing. Thus, after 107 h of annealing, the mechanical and chemical property differences between the domains and matrix have decreased while the topographic differences have increased, so that the only remaining phase contrast is due to the topography. This work is summarized in Reference 1.

Based on the annealing study of PMMA/PB system, it is difficult to isolate the individual contribution from chemical and mechanical heterogeneity towards AFM phase image contrast of PMMA/PB system. In otherwords, an understanding of the contrast variation due to chemical or mechanical heterogeneity in polymer systems can be obtained by mapping domains having different mechanical properties using phase imaging, by minimizing the chemical properties contributions to the phase signal or by mapping domains having different chemical properties using phase imaging, by minimizing the mechanical properties contributions to the phase signal. Unannealed PS/PB blend films are ideal for this investigation because, mechanically, the glassy PS

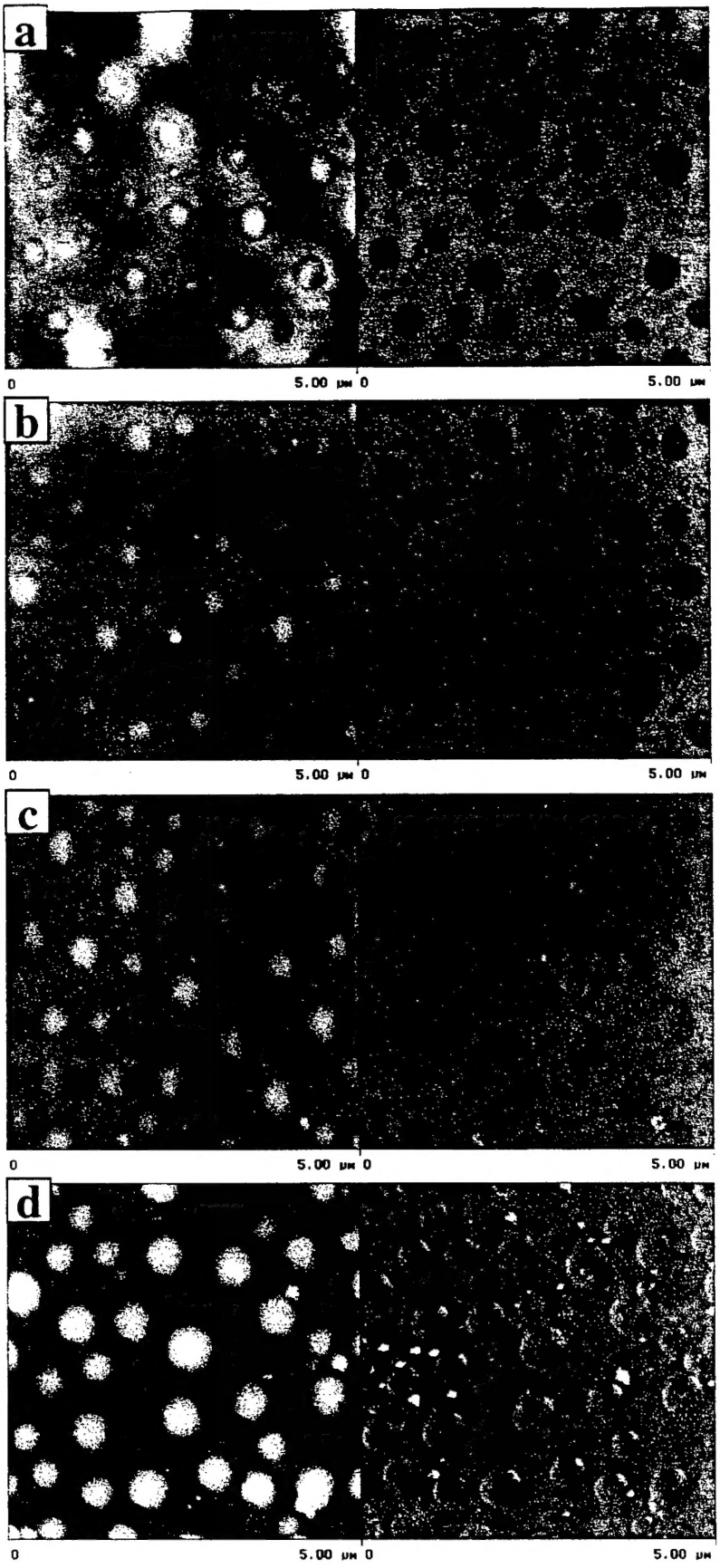

Figure 3 Tapping mode height images (left) and phase images (right) (r_{sp} = 0.88) for a 20:80 blend sample after 24 h of ambient conditioning and annealing at 75 °C ± 5 °C in air for (a) 0 h, (b) 5 h, (c) 20 h, and (d) 107 h.

material is substantially different compared to the elastomeric PB material while chemically they are similar. For example, the storage modulus, E', of unannealed PB used in this study was measured using DMA to be 1.5 MPa, which is almost three orders of magnitude lower than the value of 1.3 GPa measured for PS, while the polarities of PS and PB are similar.

In Figure 4, a 2-dimensional topographic image is shown, along with the corresponding phase image and a 3-dimensional representation of the topography, for a freshly prepared PS/PB film. The magnification of this image is indicated by the scan dimension, which is 2.5 μm. The thickness of this film was 250 nm ± 20 nm, as measured by AFM. Image analysis of lower magnification scans indicated that the bright and dark regions both occupied approximately 50 % of the sampled area. Without further analysis, however, positive identification of the dark or bright regions in Figure 1b as being PS or PB is not possible. In general, assigning chemical composition to the features observed in height and phase images is difficult unless additional experimentation is conducted. Further, the assignment of the bright or dark contrast to the hard or soft domain in phase imaging is not always straightforward. For example, several studies have assigned the brighter contrast to the stiffer material and the darker contrast to the softer material. In other reports, the darker region has been attributed to the harder material and the lighter region to the softer material. To provide further data for identifying the composition of the different regions, nanoscale indentation was performed. Using the force curve results, the dark domains in the phase image of Figure 4b were identified as consisting mostly of the glassy PS and the bright matrix consisting mostly of the elastomeric PB. Having successfully mapped the mechanically heterogeneous region systems using TMAFM and nanoindentation measurements, the next phase of the research dealt with mapping the chemically heterogeneous regions in annealed PS/PB systems.

To map chemically heterogeneous domains in a polymer system using phase imaging, the contribution due to mechanical effects must be minimized. Although PB is essentially a hydrophobic polymer, it is susceptible to thermal oxidation. When heated in air, various oxygenated groups are formed in PB and crosslinking occurs that, as was

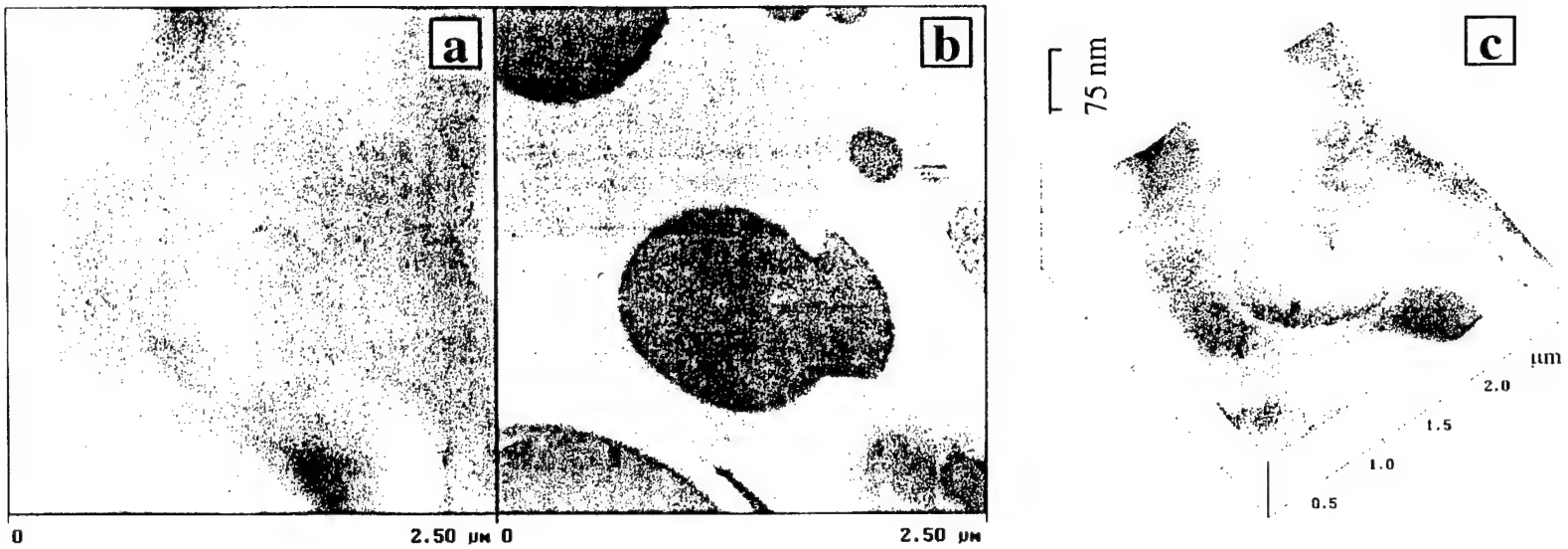

Figure 4 Tapping mode AFM height image (a), phase image (b), and 3-d image (c) of a freshly prepared 50/50 mass fraction PS/PB film on a silicon substrate. Color contrast from black to white represents a total range of 75 nm in the height image and 90 ° in the phase image.

noticed by an increase in its T_g and modulus. By adjusting the state of oxidation of the film, the mechanical properties of annealed PB was matched to that of PS while the chemical properties of annealed PB was found to be different from that of PS. By systematically changing the annealing conditions we studied the effect of annealing on the phase contrast of the PS/PB system.

In Figure 5, the height (left) and phase (right) images of a PS/PB blend film that had been annealed at 80 °C in air for several time intervals using moderate tapping are presented. Very little change in topography is observed in the height images upon annealing. The PS material continues to occupy the high domains and PB matrix occupies the valleys, and the average height variation between the two regions in the heated samples is similar to that of the conditioned but unannealed samples, approximately 60 nm. However, the contrast of the phase images greatly changes as a result of heating. Except at some edge areas, the contrast between the PS domains and the PB matrix is substantially reduced after 60 h and becomes negligible after 102 h of heating. At long heating times, the contrast difference between most of the droplets and the PS domains disappears. These results may provide qualitative insight concerning the relative contribution of the mechanical and chemical properties on the phase contrast for the PS/PB system.

In summary, using a combination of tapping mode at proper forces applied on the probe tip, nanoindentation with an AFM, and other analytical techniques, we were able to characterize the heterogeneity in the unoxidized PS/PB and PMMA/PB films at the nanoscale level. Details of this work can be found in References 1, 2, 3 and 4. Although a strong phase contrast between the mechanically heterogeneous regions in the unoxidized PS/PB film has been observed, the phase contrast between the chemically heterogeneous regions in the oxidized nonpolar PS/(polar) PB system is extremely weak and requires further investigation.

2) Characterization of Chemical Heterogeneity of Coating Model Compounds

The second phase of our investigation utilized functionalized AFM probe tips and modified samples to chemically map the hydrophilic regions in a polymer film at the nanoscale level. For this purpose, we modified the AFM probe tips and sample substrates

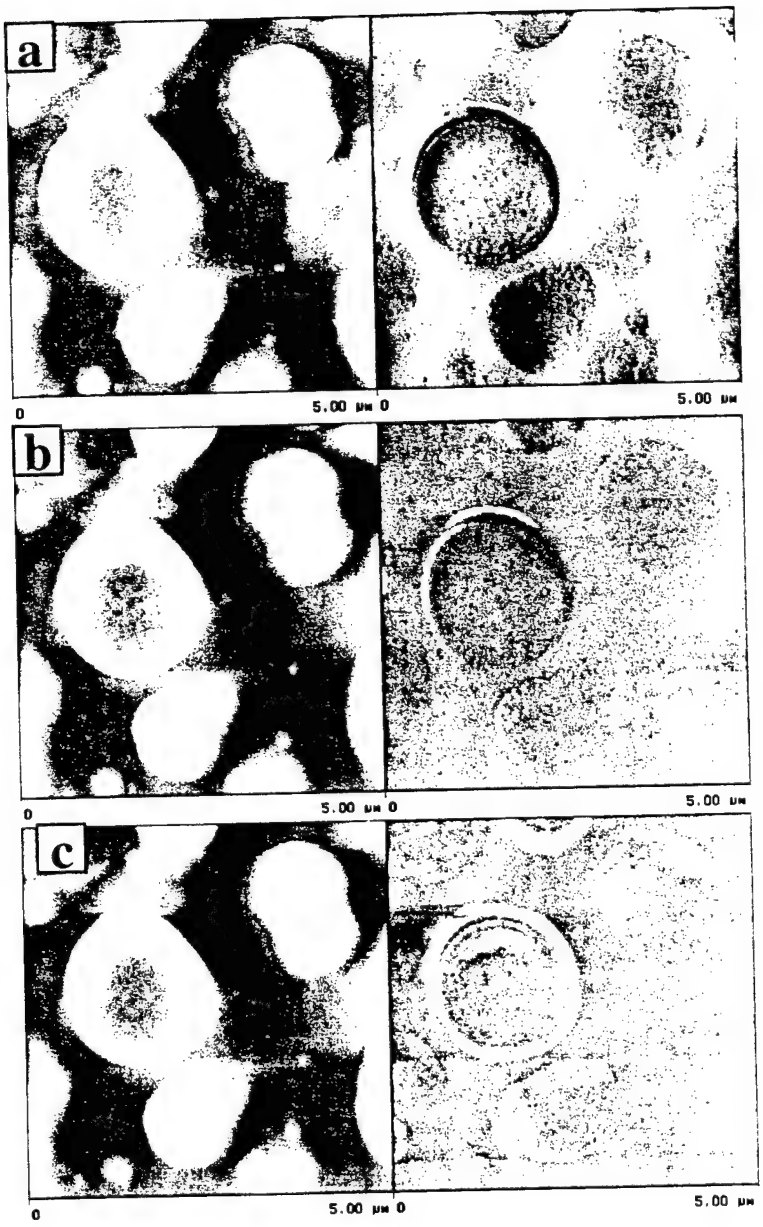

Figure 5 Height images (left) and phase images (right) using moderate tapping forces for a 50/50 mass fraction PS/PB film that had been annealed at 80 °C in air for 0 h (a), 60 h (b), and 102 h (c). Color contrast from black to white represents a total range of 75 nm in the height image and 90 ° in the phase image.

with a number of functional groups (-CH_3, -NH_2, and -COOH) based on both siloxane and thiol model compounds. The siloxane can react covalently with the Si (SiO_2) tips and Si (SiO_2) substrates while the latter are used when the tips and substrates are coated with a gold layer. Both contact mode and tapping mode AFM under different applied force levels and under different environmental conditions (N_2, dry air, and at different relative humidities) have been used for this study. Both the AFM images and force curves of these samples have been obtained.

During this phase of the research, we discovered that the presence of moisture in the sample and moisture surrounding the tip is extremely important to obtain good contrast of the hydrophilic regions in a polymer coating film using TMAFM. In this study, we used self-assembled monolayer (SAM) samples containing a lithographically-defined arrangement of hydrophilic and hydrophobic regions. The surfaces of these samples were patterned with both –CH_3 (hydrophobic) and –COOH (hydrophilic) terminating groups. Because different regions of the patterned samples have the same chain length and microstructure, any contrast observed is attributed mainly to the chemical difference between the two regions. AFM images of these samples were recorded using unmodified Si tip in a NIST-developed AFM environmental chamber (patent pending), where humidity, temperature and gas can be varied. Using this environmental chamber combined with NIST-developed, high-precision humidity generators, it is possible to provide reproducible and well-controlled relative humidities (RH) ranging from <10% to 90% surrounding the sample surface and AFM tip during the analysis. Figures 6, 7, and 8 present typical topographic and phase images of –COOH and –CH_3 terminated regions of a patterned SAM sample upon exposure to 90%, 60%, and ~10% RH, respectively. As can be seen in these figures, the phase contrast between the –CH_3 and –COOH regions decreases with a decrease in RH. Further, phase images obtained in the N_2 environment are similar to those of dry air (i.e., Figure 8). To confirm the observation that the presence of moisture plays a key role in the contrast of TMAFM phase image, the SAM sample that was exposed to the <10% RH condition was allowed to re-equilibrate in the 90% RH, and phase image was recorded again. Our results

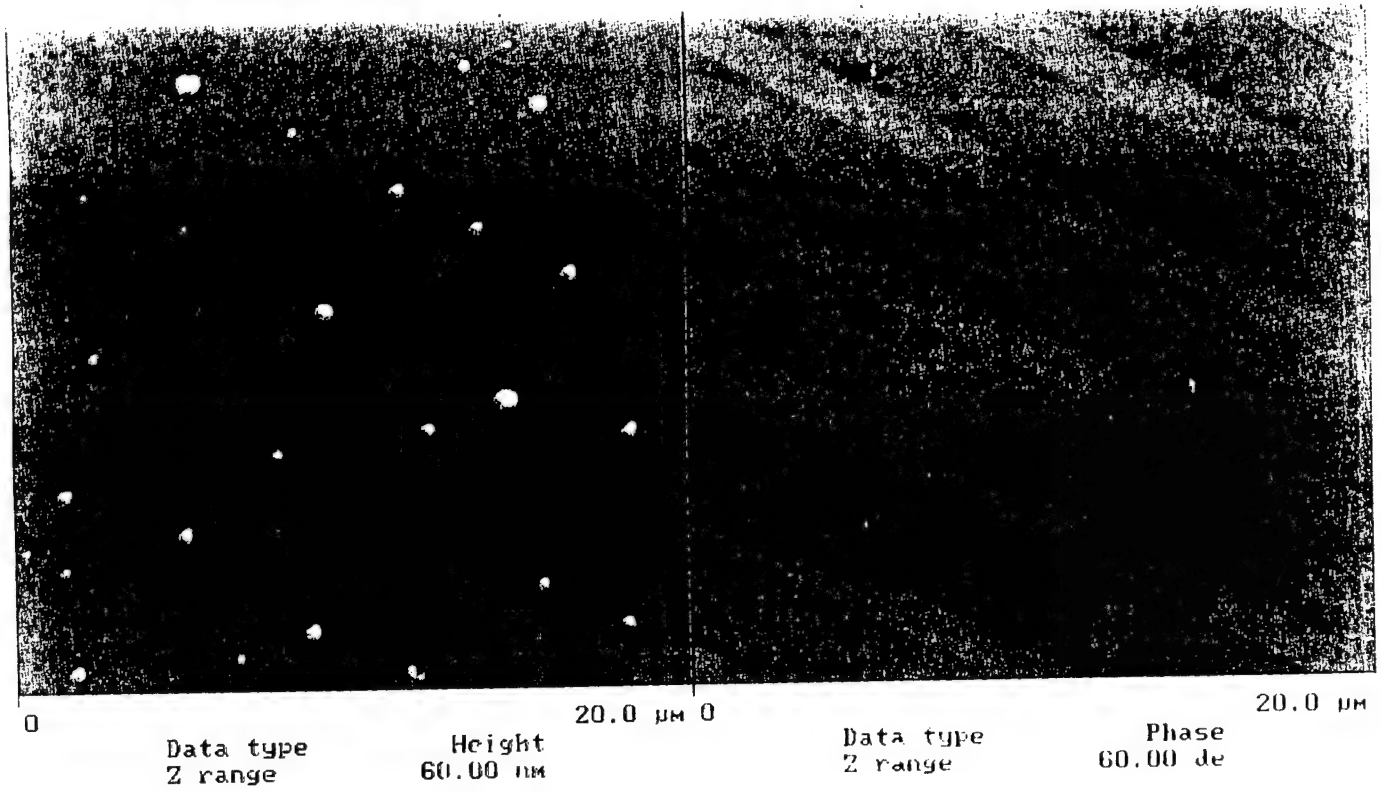

Figure 6 Tapping mode height images (left) and phase images (right) (r_{sp} = 0.68) for a SAM sample conditioned at 90% relative humidity. Contrast variations are 60 nm from white to black for the height images and 60 ° from white to black for the phase image.

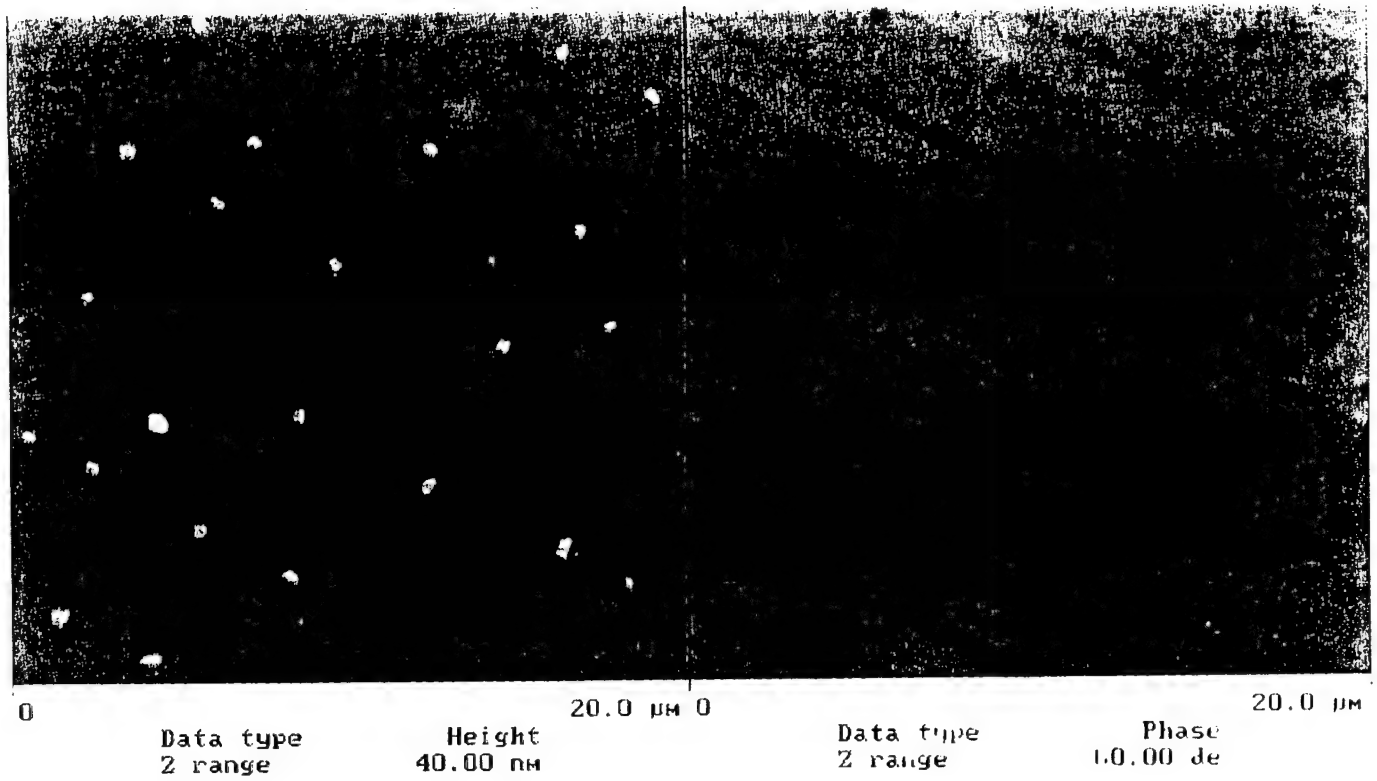

Figure 7 Tapping mode height images (left) and phase images (right) (r_{sp} = 0.65) for a SAM sample conditioned at 60% relative humidity. Contrast variations are 40 nm from white to black for the height images and 60 ° from white to black for the phase image.

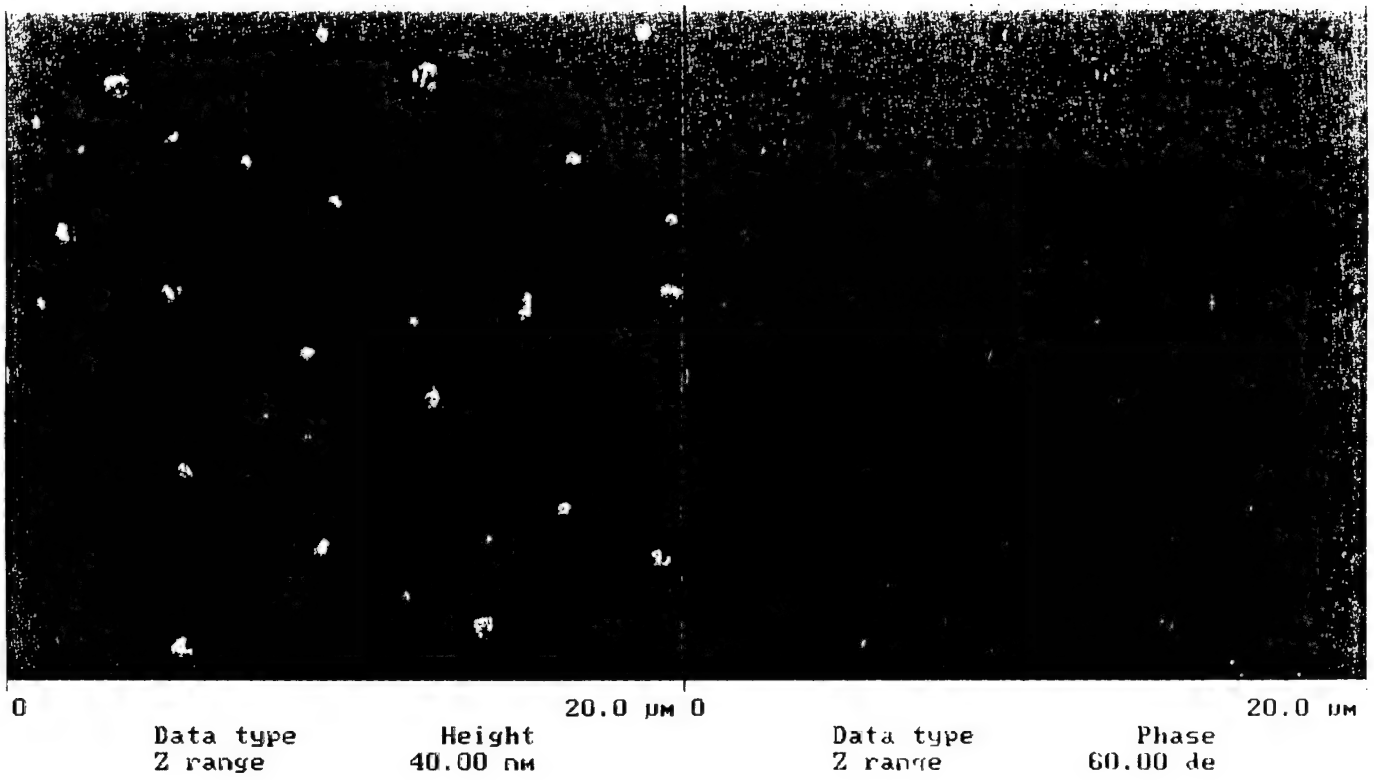

Figure 8 Tapping mode height images (left) and phase images (right) (r_{sp} = 0.65) for a SAM sample conditioned at 14% relative humidity. Contrast variations are 40 nm from white to black for the height images and 60 ° from white to black for the phase image.

highlight that the contrast was restored of the hydrophilic regions upon re-equilibrating the sample from a low RH (e.g, Figure 8) to a high RH.

The results of Figures 6 to 8 clearly show that, in the absence of moisture, even the highly hydrophilic COOH-terminated regions could not be chemically distinguished from the hydrophobic CH_3 regions in a SAM sample. (It should be noted that similar results were obtained for hydrophilic-modified tips.). Further investigation is needed for better understanding the phase image contrast enhancement in the presence of moisture. Although more substantial data are needed in order to recommend a protocol for chemically mapping heterogeneous regions in coating materials, the results obtained so far suggest that a combined use of the chemically-modified tip, a proper force level on the probe tip, and a certain amount of moisture in the area surrounding the tip and sample may provide a method to successfully map the hydrophilic regions in polymer films using TMAFM in air. The results of this work are summarized in a yet to be published Reference 5.

Another progress in the effort to chemically map the heterogeneity in polymer coatings has been the development of a computer program that allows us to obtain instantaneously the stiffness and the AFM tip/sample interactions at any location of the scanned section of the sample. This program eliminates the step of exporting the AFM data and of performing time-consuming manual analysis of the force curves to provide quantitative data on the tip/sample adhesion forces and local moduli. It should be emphasized that tip/sample interaction parameters (including capillary force due to water in the environment) play a key role in the contrast mechanism of AFM images. This program is being used extensively in our study to derive the tip/sample interactions and local moduli for a variety of unmodified and chemically-modified samples using unmodified or functionalized tips.

To differentiate the hydrophilic regions in a sea of hydrophobic polymer coating films, we have to determine what is the range of polarity difference between the hydrophilic and hydrophobic regions in a film that could be distinguished by AFM. Further, in order to establish a protocol for chemically characterizing the hydrophilic regions in polymer coatings, the role and contribution of the moisture in the environment

surrounding the tip and sample on the contrast and contrast mechanism must be addressed. For example, one critical question is that what is the moisture level required to map the ester regions in a film the same as that for another region containing COOH. or OH. or NH_2 groups? Another question: what is the combined effect of moisture in the surrounding, of force level, and of sample hydrophilicity on the AFM contrast? etc. To address these types of questions, we have selected model polymer systems for which the hydrophilicity and hydrophobicity can not only be chemically converted to more or less polar groups but is also sensitive to moisture. The system selected for this study is PS/poly(ethylacrylate) (PEA). PEA can be catalytically hydrolyzed to an acid. By keeping the morphology, thickness, and conditions for film preparation constant, and using a combination of different environmental conditions and polarity change of the hydrophilic regions in the films, questions such as those cited above were addressed.

In this study, an highly aggressive chemical medium has been chosen to effectively modify one component while keeping the other component unmodified. An inorganic acid has been chosen as the aggressive chemical medium so as to accelerate the hydrolysis of one of the hydrophilic components in a two-component polymer blend. We characterized chemically heterogeneous regions in poly(ethyl acrylate) (PEA) / polystyrene (PS) blends using AFM and studied the progressive degradation of different components in a blend at the nanoscale by AFM. The progressive degradation study would be useful in understanding the degradation modes of organic coatings exposed to aggressive environments.

In Figure 9, a 2-dimensional topographic image (left) along with the corresponding phase image (right) are shown for a 70:30 PEA/PS blend film obtained by AFM under ambient conditions (rsp =0.70). The magnification of these images is indicated by the scan dimension, which is 10 μm. The thickness of this film was 150 nm $\pm$ 20 nm, as measured by AFM. Both the phase and topographic images reveal that phase separation has occurred; the domains that appear as circular regions are of bright contrast with respect to the matrix.

To identify the domain and matrix regions as PEA-rich and PS-rich or visa versa, an attempt was made to expose the blend film to an aggressive chemical environment and

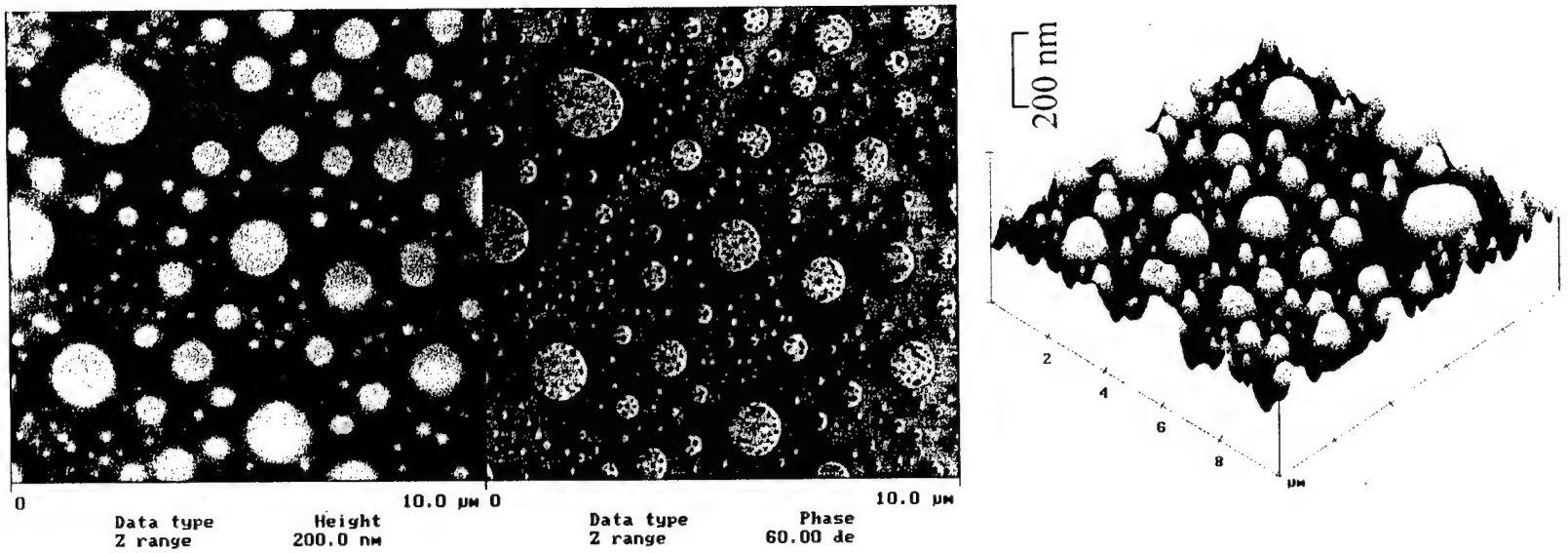

a b

Figure 9 (a) Tapping mode AFM height image (left) and phase image (right), and (b) a 3-dimensional representation of the topography for the 70:30 PEA/PS blend after 24 h of ambient conditioning (r_{sp} = 0.70). Contrast variations are 200 nm from white to black for the height images and 60 ° from white to black for the phase image.

examine the unexposed and exposed film by AFM. Figure 10a shows a 3-D topographic image of the 70:30 PEA/PS film that has been exposed to HCl vapor for 3h. The thickness of this film was approximately 150 nm ± 20 nm. as measured by AFM. Changes in the form of pits occurred in isolated regions of the matrix, but the overall morphology, size, and shape of the domains was essentially unaltered. The dark regions in the 3-D image of Figure 10a and the 2-D image of Figure 10b represent pits that are formed within the heterogeneous structure. A corresponding line profile of the sample is shown in Figure 10c, which provides the depth and width of the dark region.

To relate the changes due to acid exposure in the composition of the PEA/PS blend, PEA and PS cast films were similarly exposed to HCl vapor. The changes observed in the matrix material of the blend were assumed to correspond to changes in either the PEA or PS regions of the film with exposure to HCl vapor. Consequently, any change due to hydrolytic degradation should be noticeable in the AFM images of the PEA and PS films.

In Figure 11a, the AFM topographic image (left) and phase image (right) are shown for a 20 μm x 20 μm scan area of a 110 nm ± 10 nm thick PEA cast film that has been exposed to the same acid environment for 40 days. In contrast to the generally smooth surface of the unexposed PEA cast film, the surface of the exposed PEA film shows isolated degradation (dark spots in topographic image). Much of the degradation occurs at certain sites in the form of pits with lateral dimensions from several nanometers to several micrometers, as observed in the 3-D topographic image shown in Figure 11b. The observation of localized degradation at certain areas and not uniformly over the film surface is in good agreement with a recently published chemiluminescence observation that thermo-oxidation of polypropylene initiates at local active oxidizing centers, followed by the spreading of these centers. Similar observations have been reported for hydrolysis of a polycarbonate system. The model for this localized hydrolysis is based on the existence of water sensitive domains that behave differently from the bulk polymer structure. These domains can be polar molecules such as monomers, dimers, or catalysts that did not participate in polymerization. Although the domains are few in an unhydrolyzed polymer, they are believed to represent the initial sites of water sorption,

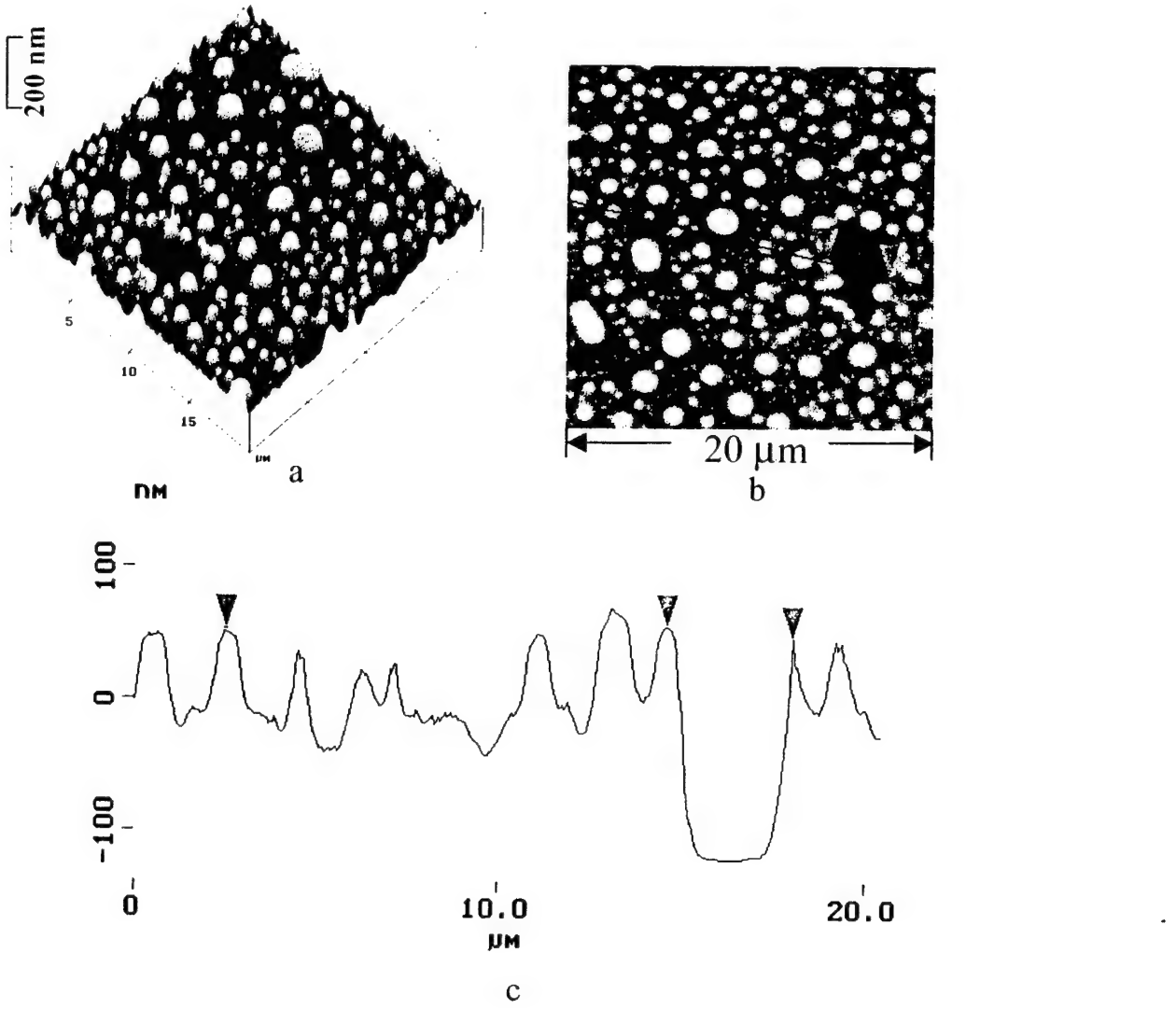

Figure 10 (a) A 3 D representation of the topography image, (b) tapping mode height images and (c) line profile for a 70:30 blend sample after 24 h of ambient conditioning and exposing the film to HCl vapor for 3h. Contrast variations are 200 nm from white to black for the height images.

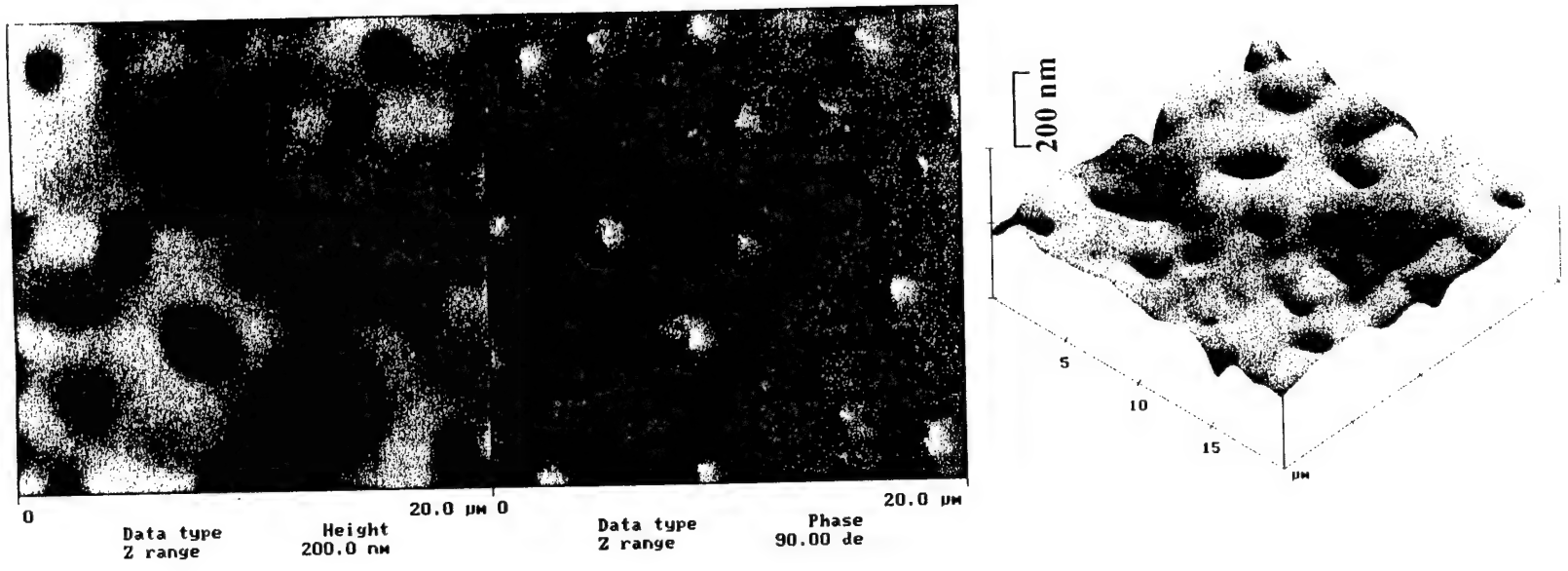

a b

Figure 11 (a) Tapping mode AFM height image (left) and phase image (right) and (b) a 3-dimensional of the topography for the PEA film after 24 h of ambient conditioning and exposing the film to HCl vapor for 40 days. Contrast variations are 200 nm from white to black for the height image and 90 ° from white to black for the phase image.

hydrolysis and degradation. As hydrolysis proceeds, the material that border the cluster of polar molecules start to degrade through dissolution and/or hydrolysis. The enhanced reactivity of localized domains is consistent with the observations of increases in the width and depth of the pits with exposure time and number of isolated pits in the hydrolyzed PEA film.

To verify that the PEA was indeed hydrolyzed during acid exposure, fresh PEA film was subjected to the same acid hydrolysis and temperature conditions (as for the blend) and the composition of the film was studied by FTIR. In Figure 12a, the FTIR transmission spectra of a spin coated PEA film on CaF_2 are shown for the region from 3800 cm^{-1} to 1200 cm^{-1} as a function exposure time to HCl vapor. Peak attributable to pure PEA is observed at 1732 cm^{-1} and is assigned to the ester C=O stretching. The difference spectra (Figure 12b) between the film exposed to different times and the unexposed film was used to measure the ester group consumption and formation of the acid group for the entire 110 $\pm$ 10 nm film thickness. Two bands that are attributable to the OH stretching (3400 cm^{-1}) and acid C=O stretching (1710 cm^{-1}) appear in the difference spectra. This indicates that acid and alcohol were formed upon hydrolysis of the PS/PEA film. From the difference spectra, the loss of ester peak and the growth of acid and alcohol peaks in the PEA film with exposure time can be clearly noticed.

Although the time scales of ester conversion, as monitored by FTIR, and that of the morphological alteration of the PEA film as studied by AFM are only qualitatively comparable, all information is consistent with hydrolysis of the PEA in the blend upon exposure to HCl vapor and dissolution of the PEA component from the blend leading to the formation of pits. The underlying conclusion from these results is that the changes observed in the PEA film correspond to the changes in the hydrophilic regions of the model coating system when exposed to HCl vapor.

With the successful identification of domains and matrix in chemically heterogeneous polymer blend, the effect of exposure time on the degradation of the 70:30 PEA: PS blend was studied. To quantify the changes in the matrix material with exposure to HCl vapor, the width and diameter of the pit in the 20 μm x 20 μm image (see Figure 10) are calculated using the AFM analysis software. In Figure 13, the

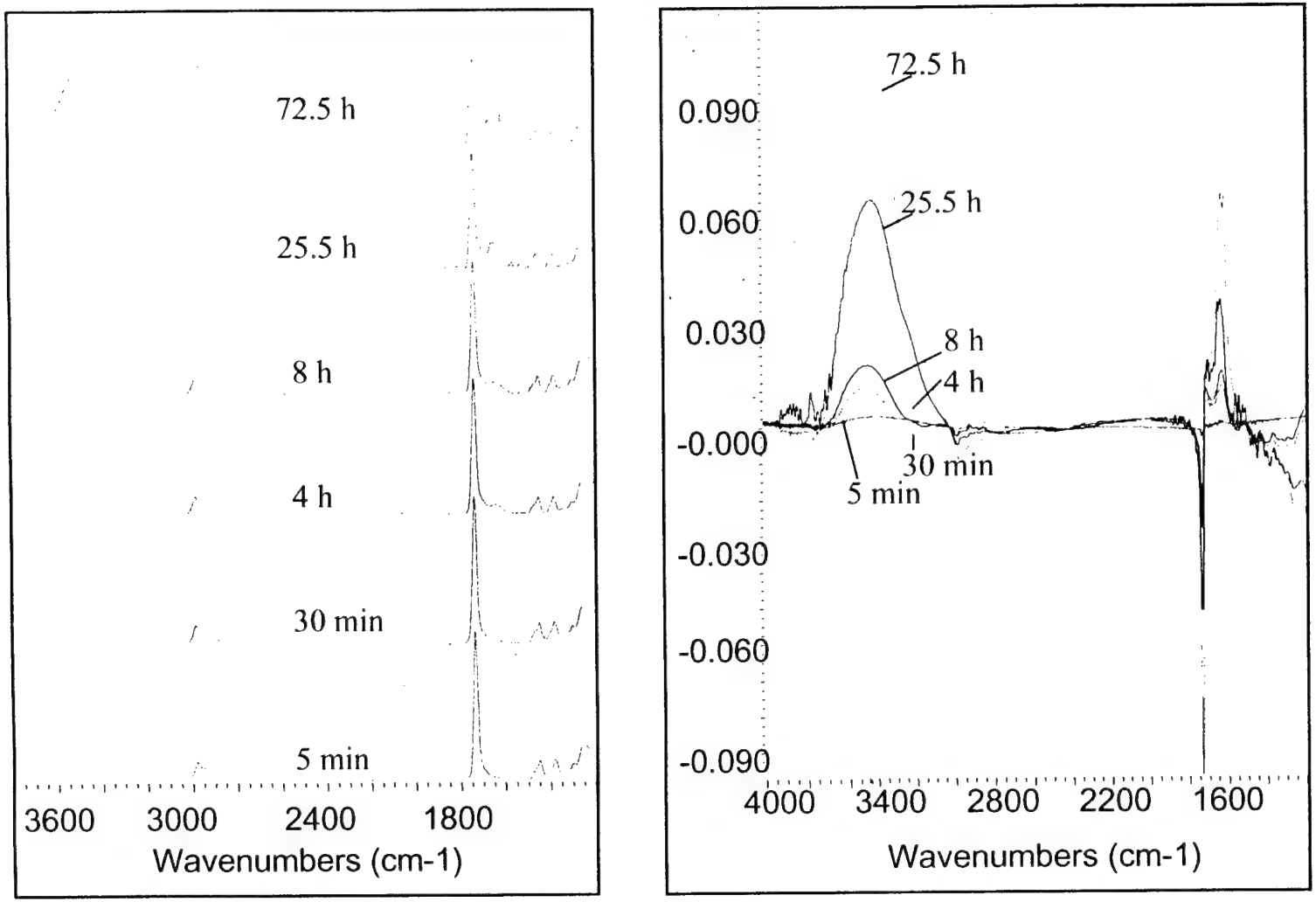

Figure 12 (a) Unprocessed and (b) difference FTIR-transmission spectra in the 3800-1200 cm^{-1} regions showing the effects of exposure of PEA film to HCl vapor .

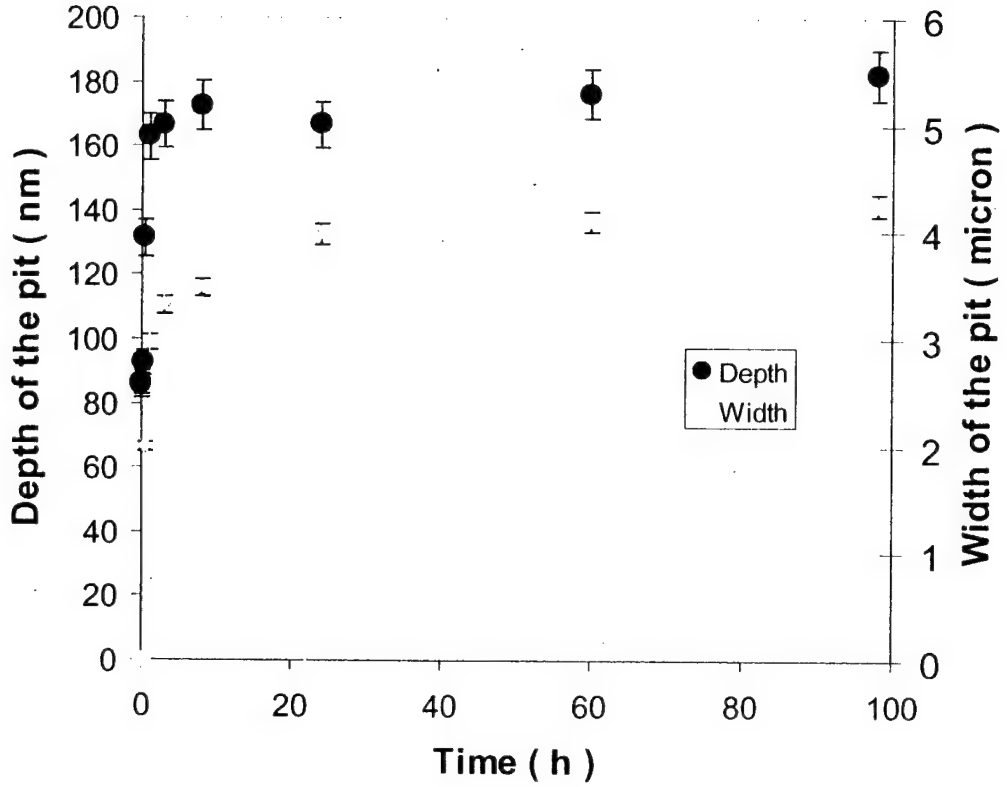

Figure 13 Changes in depth and width of a pit in a PEA/PS blend as a function of time exposure to HCl vapor at 24 $\pm$ 2°C

deepening and enlargement progression of the pit are shown as a function of time of exposure to HCl vapor. As described previously, the thickness of this film was approximately 150 nm ± 20 nm. The pit width increased rapidly reaching a value of 4.2 μm within the first 20 h of exposure and then leveled off thereafter. The depth of these pits continued to increase up to 100 nm after 100h of exposure. These results indicate that the pit not only grew laterally, but also through the thickness of the film. In fact, the pit has reached the bare silicon substrate, within a very short exposure time, as evidenced in Figure 13b in which the entire 150 nm film has been removed. The results of this work are summarized in Reference 6 and 7.

3) Nanoscale Characterization of Coating Degradation

The main objective of the final phase of this research was to provide mechanical, topographical, and chemical information of degradable regions in an exposed and unexposed polymer coating film whose dimensions are in the range from interatomic to a hundredth of a millimeter. Atomic force microscopy has been used to investigate coating surface changes due to weathering. Samples of an unpigmented acrylic-polyurethane were exposed to a well-controlled environmental chamber, where ultraviolet (UV) radiation and relative humidity were precisely varied and monitored. Using the micrometer accuracy of the AFM's sample positioning stage, a method was developed to enable the same regions of the coating sample to be imaged each time the sample was removed from the exposure environment for investigation. In addition to AFM data of surface changes, FTIR transmission spectra of the exposed samples were collected as a function of exposure time using an auto sampler, where FTIR spectra at the same site on each of the multiple samples can be collected automatically. FTIR chemical degradation data was related to AFM surface roughness changes. It is noted that FTIR is the most effective method for quantifying polymer degradation at the molecular level, and the data obtained by this method, with suitable models and a clear understanding of the degradation mechanisms, can be used to predict the service life of polymers and coatings. The effective UV dosage (dosage that causes coating degradation), coating damage, and quantum yield were calculated using a NIST-developed computer program, in which the results of these parameters can be obtained

as input data are entered. These results were used for predicting the service life of polymer coatings under different weathering conditions. Results of some of the work are discussed in Reference 8.

In these studies, unpigmented acrylic-polyurethane coating systems were exposed to a variety of conditions, including specific wavelengths of UV, no UV, and the full UV spectrum in combination with different relative humidities (including < 1 % RH). For this study, a NIST-developed calibrated solar simulator was used where humidity, temperature and wavelength of UV light can be varied. The NIST-developed software program allows to derive the effective dosage, coating damage, and quantum yield and predict the service life of uv radiated coating. The 2-dimensional topographic images are displayed in Figures 14 a-c for an acrylic polyurethane film that had been exposed to UV, humid and a combination of UV and humid environment. The dark regions in the 2-D image of Figure 14c represent pits that are formed within the heterogeneous structure. The AFM results showed that acrylic-based polyurethane coatings undergo substantial degradation and that both the extent and rate of degradation are much greater under UV and high relative humidities than under no UV with high relative humidity or UV with low humidity. Furthermore, much of the degradation occurs at certain sites in the form of pits with lateral dimensions from several nanometers to several micrometers. An attempt was made to study the growth of pit for an acrylic polyurethane film upon exposure to 90% RH and full UV (from 290 nm to 800 nm); the results were obtained by tapping mode AFM. The pit diameter rose rapidly within the first 30h of exposure and then eventually leveled off, after 100h of exposure. While, the depth of these pits continued to increase up to 400 nm after 4 months of UV and humidity exposure. The growth of pits through the coating to the substrate, resulting in pathways for moisture to travel to the substrate is believed to be the cause of substrate corrosion.

To relate the pit formation with the chemical changes of the acrylic-polyurethane film during exposure to various environments, the surfaces of acrylic-polyurethane film before and after exposure were characterized by attenuated total reflectance Fourier transform infrared spectroscopy. In order to make a comparison between the samples subjected to different exposure, the intensity of each peak was ratioed against the

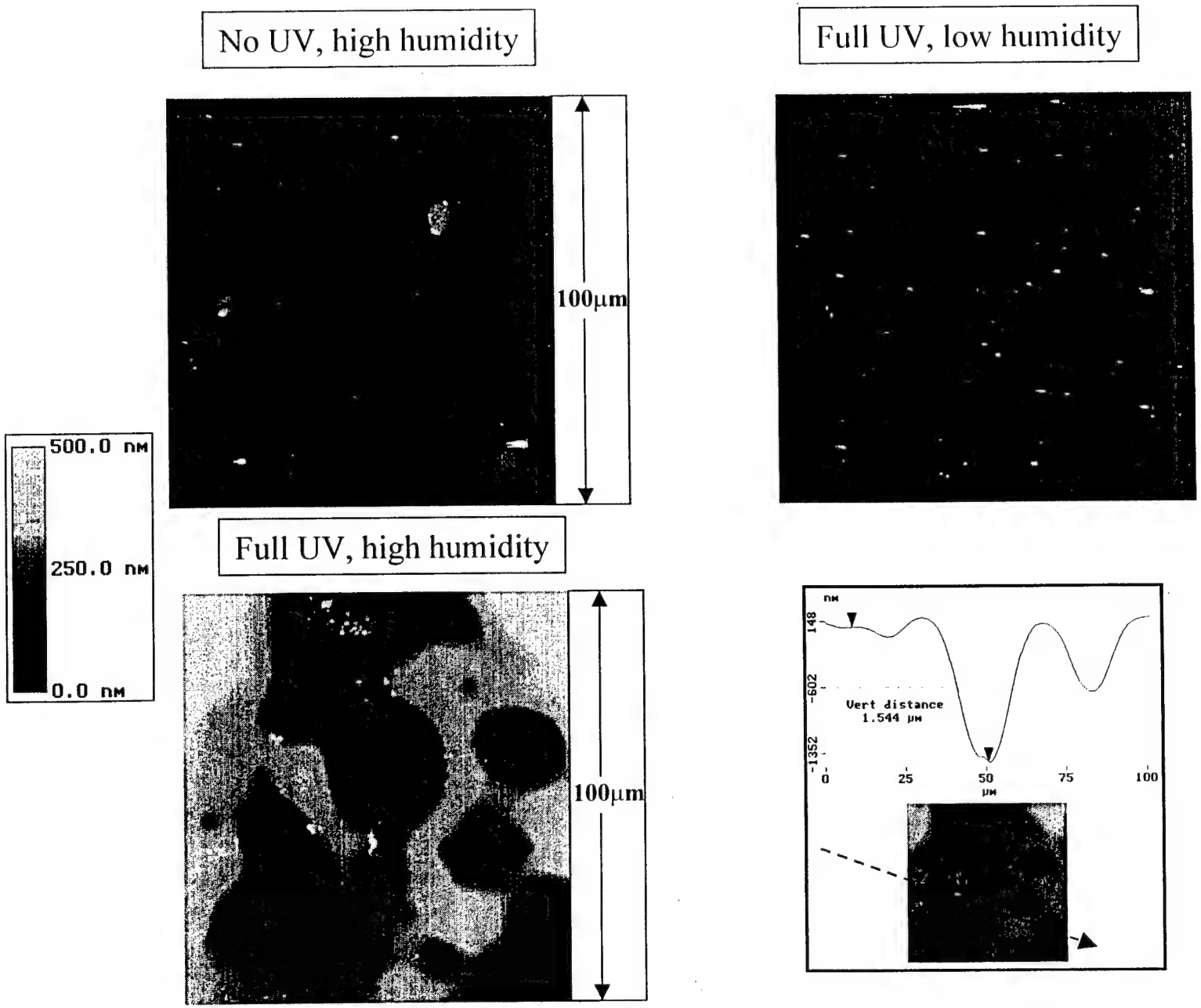

Figure 14 Tapping mode height image of (a) UV exposed (b) moisture exposed and (c) moisture and UV exposed and (d) line profile of Figure 14c for a acrylic urethane film. Exposure time is 6250h, 100% RH, and 100% UV range.

absorbance of a band whose intensity does not change. The difference in absorbance were then obtained by subtracting the integrated intensity absorbance of normalized spectra of a region of interest at a specified period from that of the unexposed sample. One of the typical band of acrylic-polyurethane film, which can be attributed to the NH bending at 1520 cm^{-1} was found to decrease in absorbance intensity upon exposure to various environments. During exposure of acrylic urethane film, the absorbance intensity of another band attributed to CO stretching at 1748 cm^{-1} increased, indicating that oxidation has occurred in the film. Figures 15-16 represent the plot of NH intensity and CO intensity of acrylic-polyurethane film as a function of exposure time in various environments. The decrease in the intensity of NH peak in the exposed acrylic-polyurethane film is a result of chain scission in the acrylic urethane film. A photodegradation mechanism in which the urethane crosslinks undergo scission in the presence of UV light and oxygen environment to form hydroperoxide intermediate is consistent with proposed mechanism for degradation of acrylic urethane film. The intermediate through cage reaction eventually forms acetyl urethane. The formation of acetyl urethane, is indicated by the increase in absorbance intensity of CO band at 1752 cm^{-1}. The acetyl urethane can decompose in the presence of moisture to form acid and urethane. From the FTIR results, it can be concluded that the exposure of organic coatings to UV and relative humidity has caused significant chain scission and oxidation of the film. FTIR results support the AFM observation (pit formation) that the extent of degradation is much larger for samples exposed to UV at high relative humidities compared to other conditions.

The other aspect of the research was to study the composition of the degradation-susceptible regions in a polymer coating. In this study, an unpigmented polyester coating was immersed in an alkaline environment (to accelerate hydrolysis) at ambient temperature. Figure 17 shows the topographic and phase TMAFM images of unexposed polyester film. A heterogeneous structure is clearly observed on length scales less than 1mm in both topographic and phase image. A detailed explanation of the heterogeneous structure observation in polyester film can be found in References 9 and 10. Figure 18 shows the topographic and phase images of film that had been

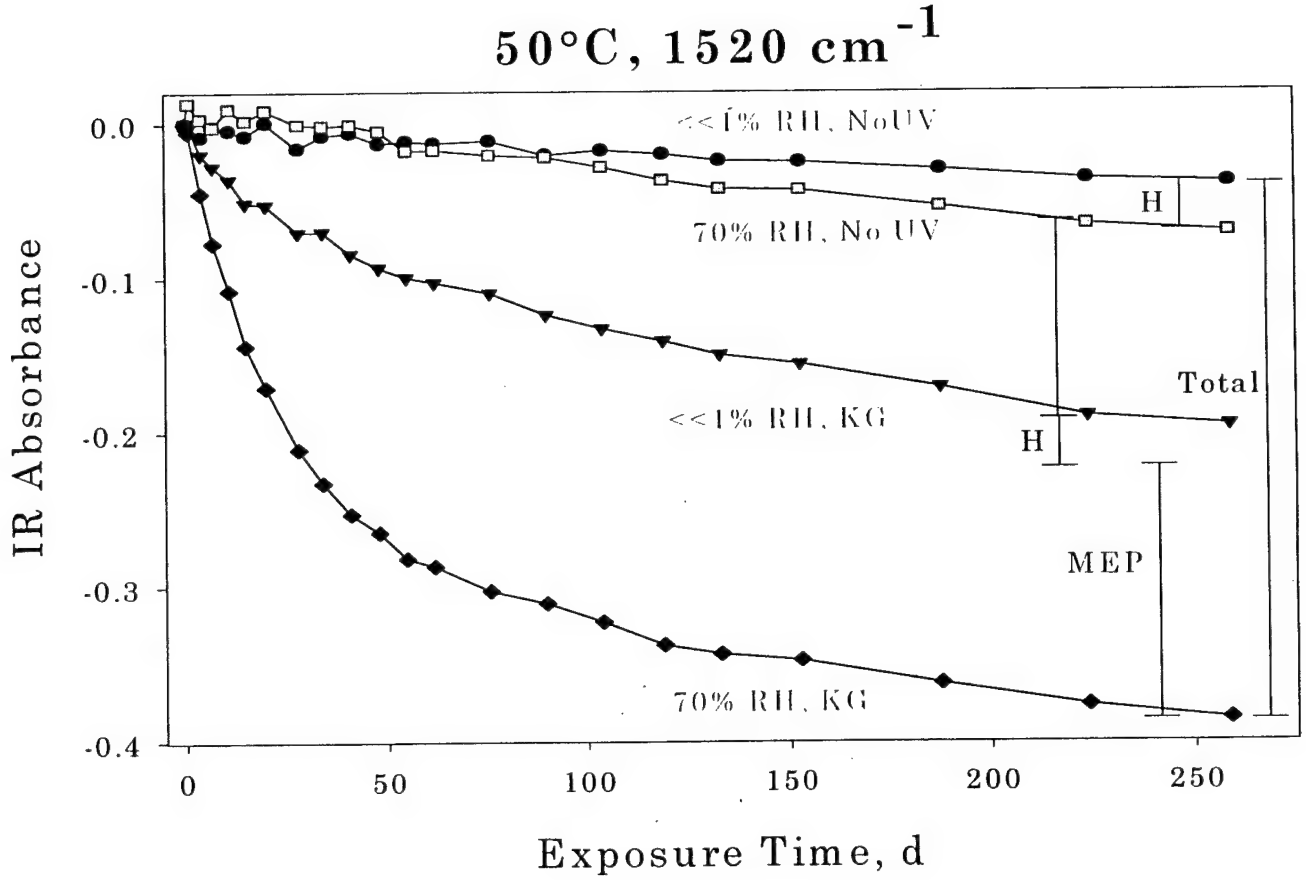

Figure 15 The intensity change of NH peak at 1520 cm^{-1} of a polyurethane film as a function of exposure

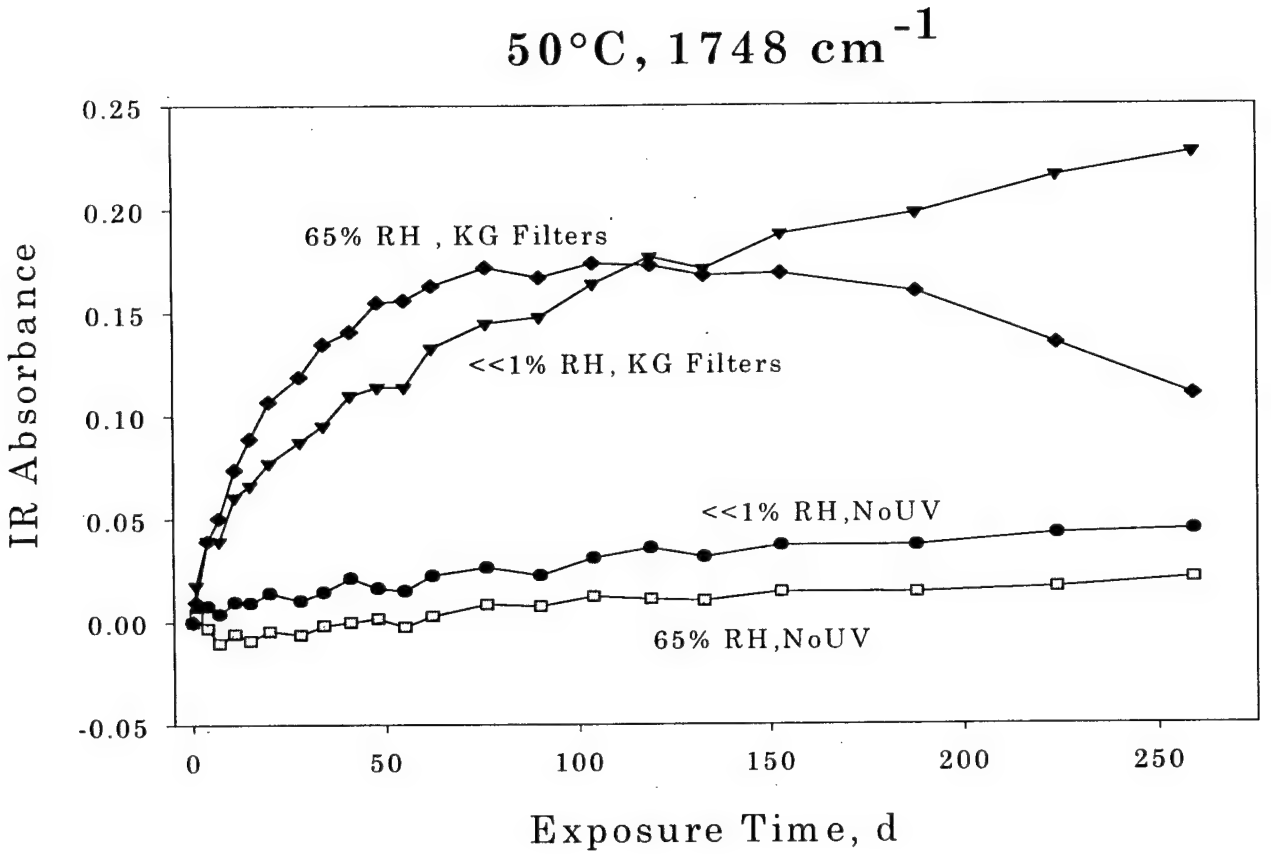

Figure 16 The intensity change of CO peak at 1748 cm^{-1} of a polyurethane film as a function of exposure.

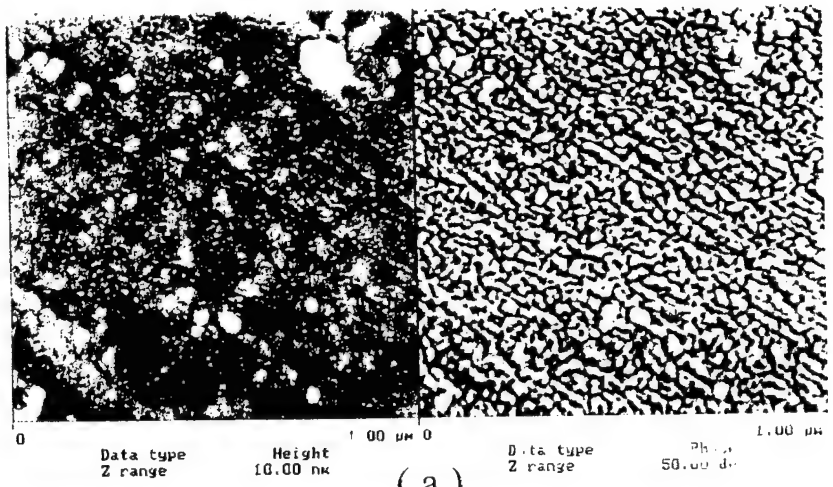

Figure 17 Tapping mode AFM height image (left) and phase image (right) of the unexposed polyester film. (a) 1 x 1µm and (b) 500nm x 500 nm. Contrast variations are 10 nm from white to black for the height image and 50 ° from white to black for the phase image.

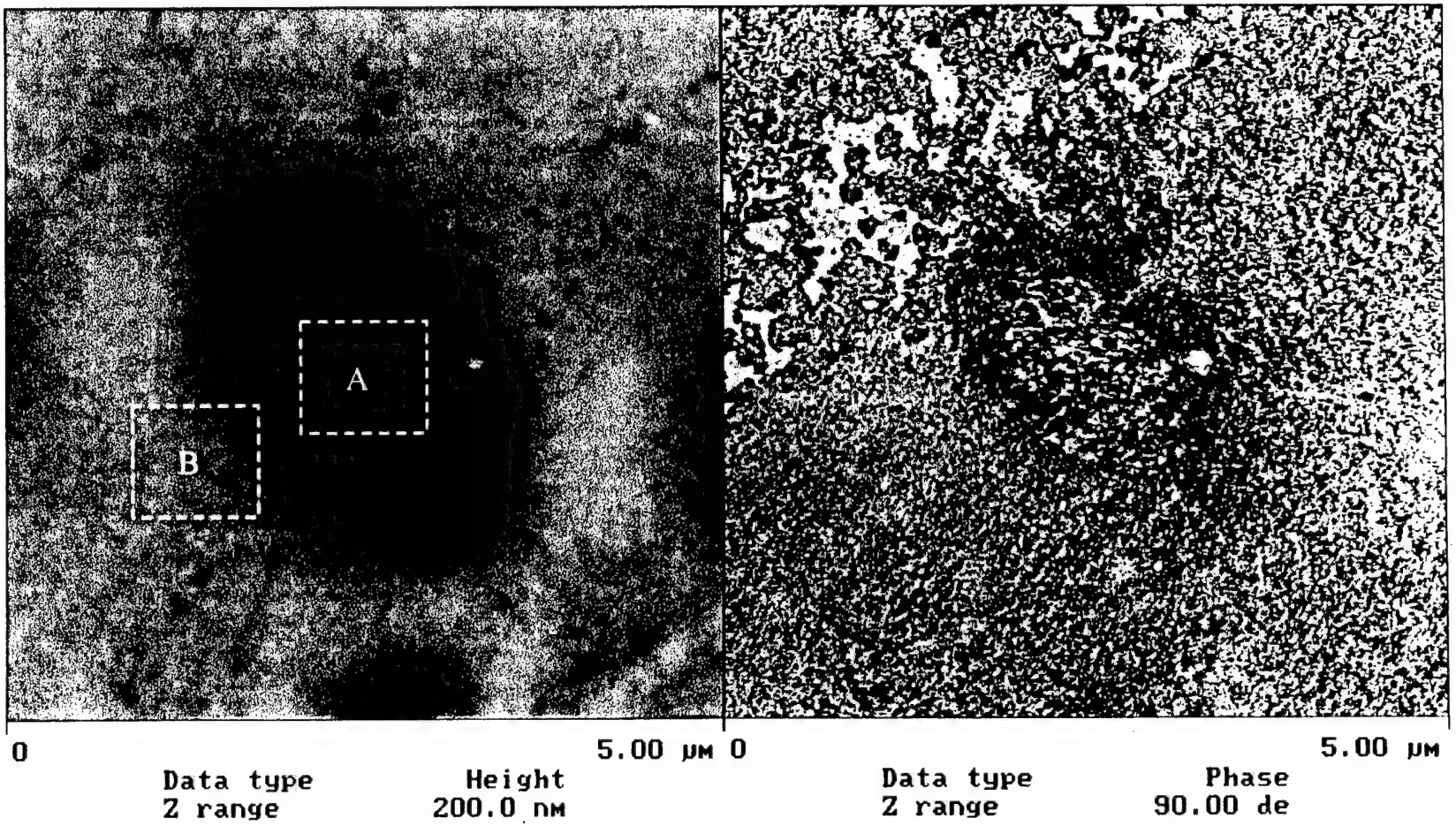

Figure 18 Tapping mode AFM height image (left) and phase image (right) of the polyester film exposed to 3M NaOH solution for 28 days. Contrast variations are 200 nm from white to black for the height image and 90 ° from white to black for the phase image.

exposed for 28 days. The microstructure of the polyester film was substantially changed after exposure. More and deeper pits were observed on the sample surfaces with increasing exposure time. Phase imaging indicated that the properties of the regions with the degradation pits are significantly different from those of the undegraded regions.

To estimate the difference in the mechanical/adhesive properties between the regions with and without pits, force curves were recorded on the bright colored region in an unpitted area and on the dark-colored region inside a pit; these results are shown in Figure 19a-b. Although providing absolute values for the elasticity and the adhesion force is difficult, the behavior in different regions of the same sample can be compared from the force curves. As can be seen, much larger hystersis between the loading and unloading curves is observed in Figure 19b compared to Figure 19a. The loading curve in Figure 19a indicates that it is hard for the utilized tip to penetrate in to the bright regions, while in Figure 19b the tip initially penetrated into the sample for 100 nm, then it started to touch the stiff material that it could not penetrate. These observations indicate that the surface of the dark-colored region might be more plastic or adhesive than that of the bright-colored region. Thus the degraded regions within the pits may have properties different from the unpitted region.

In addition to characterizing the degraded film, the material leached out from the coating was analyzed by total organic carbon, FTIR, and liquid chromatography-mass spectrometry. Total organic carbon analysis of the leached aqueous medium showed the presence of organic compounds, suggesting a chemical degradation of the film in the alkali medium. The FTIR spectrum of the organic extract medium is shown in Figure 20(b). The spectrum of the disodium salt of isophthalic acid is also shown in Figure 20(a). Signature peaks of the monomer (acid salt) used in the polyester formulation were noticed in the spectra of the extract. FTIR analysis support the evidence for the formation of carboxylate species upon degradation of polyester film in alkali solution. LC/MS analysis of the leached medium confirmed the presence of isophthalic acid and sodium isophthalate. These results revealed that the materials leached out from the films during immersion were mostly unreacted starting monomers

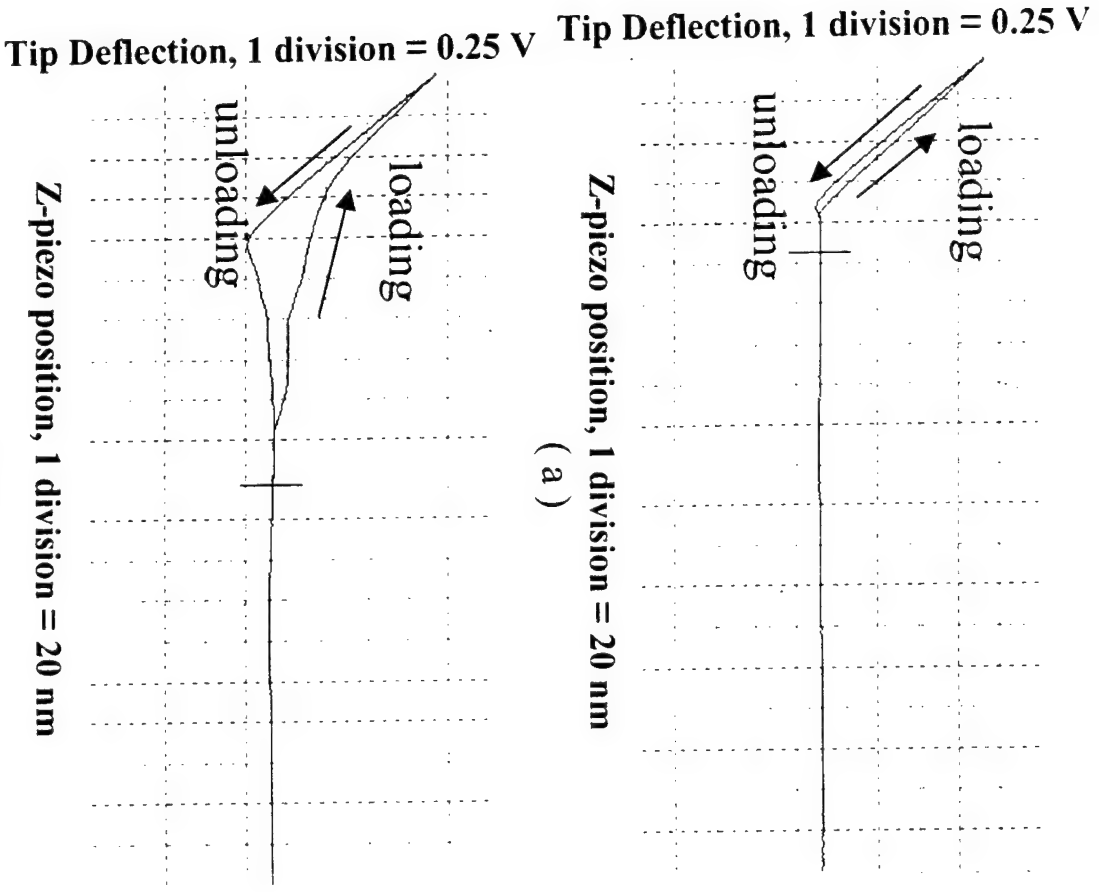

Figure 19 Typical force curves for (a) the bright-colored region and (b) the dark colored region inside the pit.

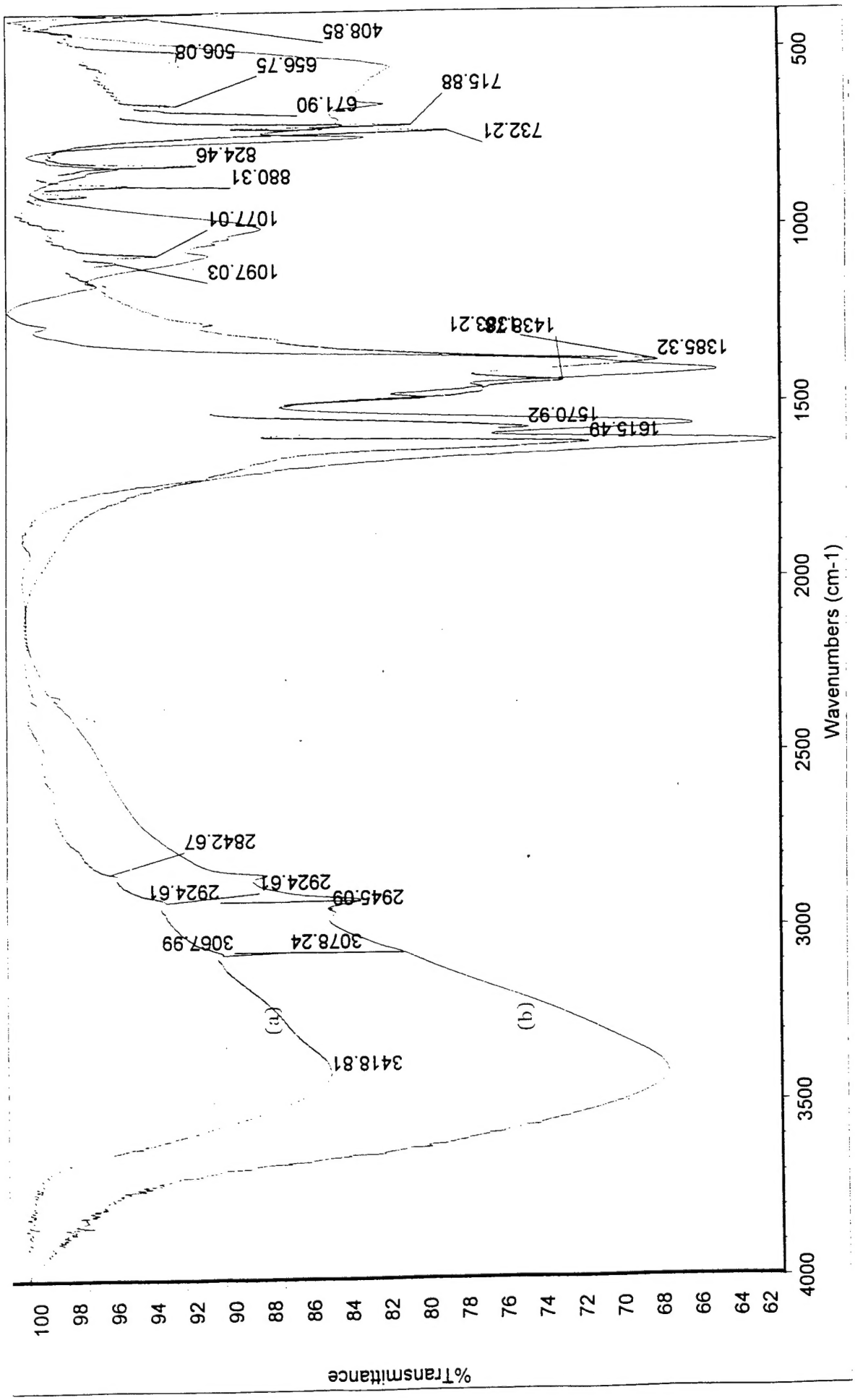

Figure 20 FTIR spectrum of (a) salt of isophthalic acid and (b) extract from polyester film.

and oligomers. We believe that most of the molecules present in the leachate might have originated from the degradation susceptible regions in the coatings that are particularly prone to degradation. The results of this work are summarized in References 11 and 12.

The cause of the formation of these localized pits in polyurethane and polyester film and upon exposure to weathering environments is unknown at this time. Based on indirect evidence presented in the literature and from our own studies on acrylic based polyurethane and polyester, the presence of surface moisture along with corrosive chemicals / radiation appear to significantly enhance degradation rates of film. Thus, degradation susceptible regions may be moisture sensitive regions in a sea of a hydrophobic coating. They may be associated with locally high surface moisture levels relative to the rest of the coating. Consequently our study provides direct evidence for the existence of hydrophilic regions in polymer coating film.

In summary, with a strong collaboration with NIST and the availability of its state-of-the art research facility and expertise, we have made great progress within the last three year in the effort to map mechanically and chemically heterogeneities in model polymer systems and to characterize coating degradation at a nanoscale. In addition to the publications listed below, major accomplishments of research in the past 3 years include:

1) Characterized the degradation of polymer coatings with nanoscale lateral resolution using AFM; pits were observed to form at certain locations in the film, presumably at the degradation-susceptible regions.
2) A technique was developed which allows AFM images to be collected at the same location of the sample.
3) A protocol and a computer program were developed to quantify chemical degradation of coatings, effective dosage of UV light, and quantum yield.
4) Developed nanoindentation procedure in combination with TMAFM to identify soft and hard regions in a heterogeneous polymer system. Appropriate procedures for identifying and mapping chemically heterogeneous regions in model systems using chemically-modified tips have been established. A computer program was

developed to automatically calculate local stiffness and AFM tip/sample interactions.

5) AFM/chemical modification approach was found to be highly useful for identifying different phases in chemically heterogeneous polymer model coating system.
6) With the use of an atomic force microscope (AFM), which provides nanometer spatial resolution and angstrom depth resolution, we recently observed the progression of pathway formation in polyester and acrylic-polyurethane coatings. common protective materials for industrial, automobile, and aerospace applications.
7) An effort was made to relate the microstructure of polymer coating film to the changes that occur to film upon environmental exposure and relate the changes to the chemistry of degraded compound.
8) FTIR and AFM results (pit formation) support the observation that the extent of degradation of polymer coating film is much larger for samples exposed to UV at high relative humidities compared to no UV and high relative humidities or UV with low humidity.

Finally the procedures and methodologies developed so far can be highly useful for studying the characteristics of aircraft coatings exposed to weathering conditions. Major economic incentives exist for addressing the long-term performance of polymer coatings.

References:

1. D. Raghavan, M. VanLandingham, X. Gu, and T. Nguyen, Langmuir, (accepted) 2000.
2. M. VanLandingham, X. Gu, D. Raghavan, and T. Nguyen, Proceedings of Microscopy and Microanalysis, Portland, OR, 1999, 962.
3. D. Raghavan, X. Gu, T. Nguyen, M. VanLandingham, and A. Karim, Macromolecules, 33(7), 2573(2000).
4. X. Gu, M. VanLandingham, D. Raghavan, and T. Nguyen, Poly. Mat. Sci. Eng. 82, 50(2000).
5. M. VamLandingham, X. Gu, T. Nguyen, J. Martin, and D. Raghavan, Data to be published.

6. D. Raghavan, X. Gu, M. VanLandingham, and T. Nguyen, Journal of Polymer Science : Polymer Physics Edition, submitted (2000).

7. D. Raghavan, X. Gu, M. VanLandingham and T. Nguyen, Polym. Prep., 43(2000).

8. T. Nguyen, M. VanLandingham, X. Gu, M. Giraud and D. Raghavan, The First International Conference on Scanning Probe Microscopy of Polymers, Santa Barbara, CA, 1999, 48.

9. X. Gu, D. Raghavan, T. Nguyen and M. VanLandingham, Polymer Materials Science and Engineering, 83, 336(2000).

10. X. Gu, D. Raghavan, M. VanLandingham, and T. Nguyen, Polymer Degradation and Stabilization, submitted (2000).

11. D. Raghavan and K. C. Egwim, J. Appl. Polym. Sci. 78, 2000 (2000).

12. T. Nguyen, J. Chin, D. K. Aouadi, and D. Raghavan, Poly. Mat. Sci. Eng. 83, 319(2000).